Geol. Mag. **142** (*6*), *2005, pp. 637–649. © 2005 Cambridge University Press*
doi:10.1017/S0016756805001172 *Printed in the United Kingdom*

Information about open-system magma chambers derived from textures in magmatic enclaves: the Kameni Islands, Santorini, Greece

M. B. HOLNESS*, V. M. MARTIN & D. M. PYLE

Department of Earth Sciences, University of Cambridge, Downing Street, Cambridge CB2 3EQ, UK

(*Received* 25 November 2004; *accepted* 24 May 2005)

Abstract – Post-caldera eruptions of Santorini, Greece, over the past 3000 years resulted in the formation of the Kameni Islands, which comprise a series of compositionally similar dacitic lava flows. Each lava flow has a distinct population of partially-crystalline mafic enclaves, which we propose were derived from the break-up of a layer of replenishing magma responsible for triggering the eruption. Five of the recent flows (erupted in 1570, 1939, 1940, 1941 and 1950) include enclaves of essentially identical andesitic bulk compositions, which formed by crystallization of originally aphyric melts prior to eruption. Detailed examination of angles subtended at the junctions between pairs of plagioclase grains demonstrates that enclaves from each flow have a characteristic textural signature, with distinct differences in the extent of quench-related modification of the original population of dihedral angles formed by impingement of growing grains. These variations suggest that the temperature difference between the host dacite and the replenishing andesite at the time of layer overturn and eruption differed between flows. The uniformity of major element compositions of both the replenishing magma and the host dacitic lava flows demonstrates that the critical parameter in determining the timing of layer-overturn is the pre-eruptive H_2O content of both host dacite and replenishing magma. We suggest that the replenishing magma responsible for two of the three eruptions in the period 1939–1941 was significantly wetter than that responsible for the later 1950 eruption. The enclaves with the least amount of quench-related modification occur in the 1570 flow. We suggest that in this case the intruding magma was relatively dry.

Keywords: Santorini, magma chamber, universal stage, petrography, dihedral angle.

1. Introduction

Current models for magmatic plumbing systems under long-lived and predominantly silicic volcanoes usually incorporate a complex series of linked regions in which magma stalls on its way to the surface (e.g. Murphy *et al*. 2000; Blundy & Cashman, 2001). Thus, during ascent, magma will undergo a series of fractionation episodes driven either by cooling or decompression and degassing (Blundy & Cashman, 2001). The magma which is eventually erupted from such long-lived systems is generally expected to have resided for a significant period in a shallow part of the system (e.g. Reagan *et al*. 2003; Hawkesworth *et al*. 2004). One important trigger for eruption in such long-lived systems is thought to be the arrival from deeper in the system of a fresh batch of hotter, more primitive, magma into this uppermost chamber (e.g. Sparks, Sigurdsson & Wilson, 1977; Pallister, Hoblitt & Reyes, 1992; Eichelberger, 1995; Murphy *et al*. 2000). Understanding the eruptive behaviour of silicic volcanoes is thus heavily dependent on developing an understanding of the evolution of shallow magma chambers after replenishment. Here we present a new set of textural observations which demonstrate the important role of magma H_2O content in controlling the dynamics of replenishment-induced volcanic eruptions.

* Author for correspondence: marian@esc.cam.ac.uk

2. Previous work

2.a. Models for open-system shallow magma chambers

In a long-lived magmatic plumbing system, batches of hot, more primitive, magma may intrude into cooler, more evolved magma at shallow crustal levels. The effects of this include heating and remobilization of the cool magma (e.g. Murphy *et al*. 2000; Couch, Sparks & Carroll, 2001). Heating of the resident magma may also result in volatile release which can contribute to chamber over-pressurization and eruption (e.g. Huppert, Turner & Sparks, 1982).

Among other factors, the extent of mixing of a relatively dense replenishing magma with the host depends on the temperature of the resident and influent magmas, the contrasts in magma density and viscosity, and on the flow rate of the replenishing magma (e.g. Sparks & Marshall, 1986, Turner & Campbell, 1986). For example, forceful injection of dense replenishing magma

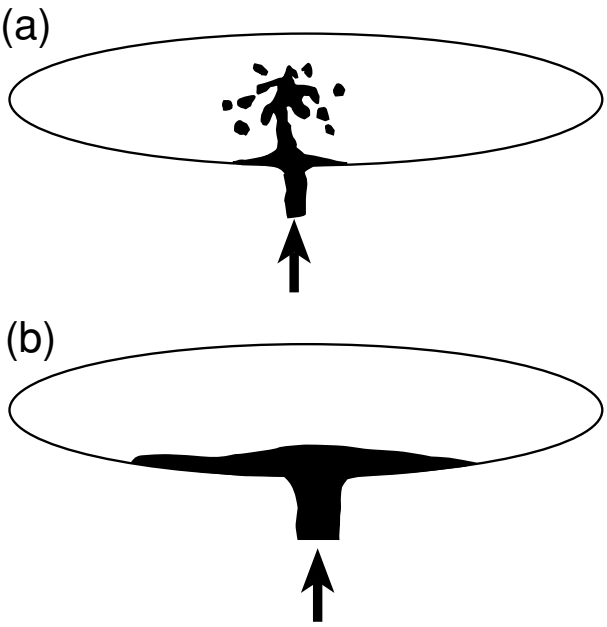

Figure 1. (a) Fountaining of replenishing magma results in the formation of mafic enclaves with chilled margins. (b) For a slower flow of replenishing dense magma, a stably stratified layer is formed at the base of the chamber. Enclaves formed as a consequence of later break-up and entrainment of this layer do not have chilled margins.

will form a turbulent fountain on entering the chamber if it has a Reynold's number > 400 (Fig. 1a; Turner & Campbell, 1986; Campbell, 1996). This fountain may then rapidly disaggregate into discrete blebs within the host, visible as mafic enclaves in the erupted lava (Coombs, Eichelberger & Rutherford, 2002).

If the Reynolds number is lower, and the rate of magma influx is low, the replenishing magma may flow along the floor of the chamber to form a stably stratified layer beneath the host (Fig. 1b; Huppert & Sparks, 1980; Huppert, Turner & Sparks, 1982; Snyder & Tait, 1995, 1996; Coombs, Eichelberger & Rutherford, 2002). Cooling and crystallization of the intruding magma will then occur, associated with exsolution of H_2O from wet magmas, as the layer cools and approaches thermal equilibrium with the resident magma. If much, or all, of the exsolved volatile phase remains trapped within the replenishing layer, the bulk density of the layer will decrease. Once the density has decreased to that of the host, mixing may occur if the replenishing layer has not yet crystallized sufficiently to form a rigid and immobile mass. This mixing will take the form of upwelling of the less dense, vesicular, partially crystalline layer into the denser overlying layer. The form of the upwelling will depend on a variety of parameters (notably the ease with which bubbles may or may not move freely through the crystallizing lower layer), and may involve the formation of discrete bubble-rich trains of vesiculated mafic magma, rising from the interface, or wholesale overturn (e.g. Thomas, Tait & Koyaguchi, 1993; Thomas & Tait, 1997; Phillips & Woods, 2002). Expansion of the gas in the vesicles in response to a pressure reduction will drive further upwelling, and could contribute to the triggering of an eruption. Vesicle expansion on uplift will also result in break-up of the layer. If layer break-up is not complete, then the erupted magma will contain enclaves which typically contain abundant glass and vesicles, but lack the chilled margins expected for enclaves formed by magma fountaining (e.g. Bacon & Metz, 1984; Coombs, Eichelberger & Rutherford, 2002).

2.b. Textural development of the crystallizing replenishing layer

When a layer of hot, relatively primitive magma is intruded into the base of a chamber dominated by a cooler liquid, cooling from both the upper and lower surfaces will drive crystallization. For magma compositions in which the primary crystallizing phases have a similar density to that of the residual liquid (and thus in the absence of gravitational settling), these crystals will grow to form a touching framework. Such frameworks are thought to have formed in liquids containing as little as 25 vol. % solids (Philpotts *et al*. 1999). If crystal growth occurs at rates significantly more rapid than that of textural equilibration, the pore geometry and connectivity in the resultant crystal framework is controlled by the orientation of impinging grains (Fig. 2a). This is known as an impingement texture, and can be recognized by the dominance of growth forms of the solid phases, and by the population of apparent dihedral angles developed at pore corners (Holness, Cheadle & McKenzie, 2005).

Crystal shapes controlled by the kinetics of growth tend to be bounded by planar surfaces (although these may be unstable relative to cellular forms such as dendrites: Lofgren, 1974; Tiller, 1991; Jamtveit & Andersen, 1992). The apparent dihedral angles developed at pore corners in an aggregate of randomly oriented crystals will form a population with a median of $\sim 60^\circ$ (Elliot, Cheadle & Jerram, 1997; Holness, Cheadle & McKenzie, 2005) with a standard deviation in the range 25–30°. Such a population is distinct from that of dihedral angles in a texturally equilibrated pore structure which has a lower median (of $\sim 30^\circ$) and a standard deviation of 13–14° (e.g. Laporte, 1994; Toramaru & Fujii, 1986; von Bargen & Waff, 1988; Waff & Bulau, 1979; Faul, 1997; Holness, Cheadle & McKenzie, 2005). This dihedral angle population is associated with more rounded crystal shapes, indicative of at least some approach to the equilibrium crystal form.

In undisturbed solidifying systems, the actual pore geometry, and thus the distribution of dihedral angles in any given sample, depends on the relative importance of crystal growth and textural equilibration. In most cases,

https://doi.org/10.1017/S0016756805001172 Published online by Cambridge University Press

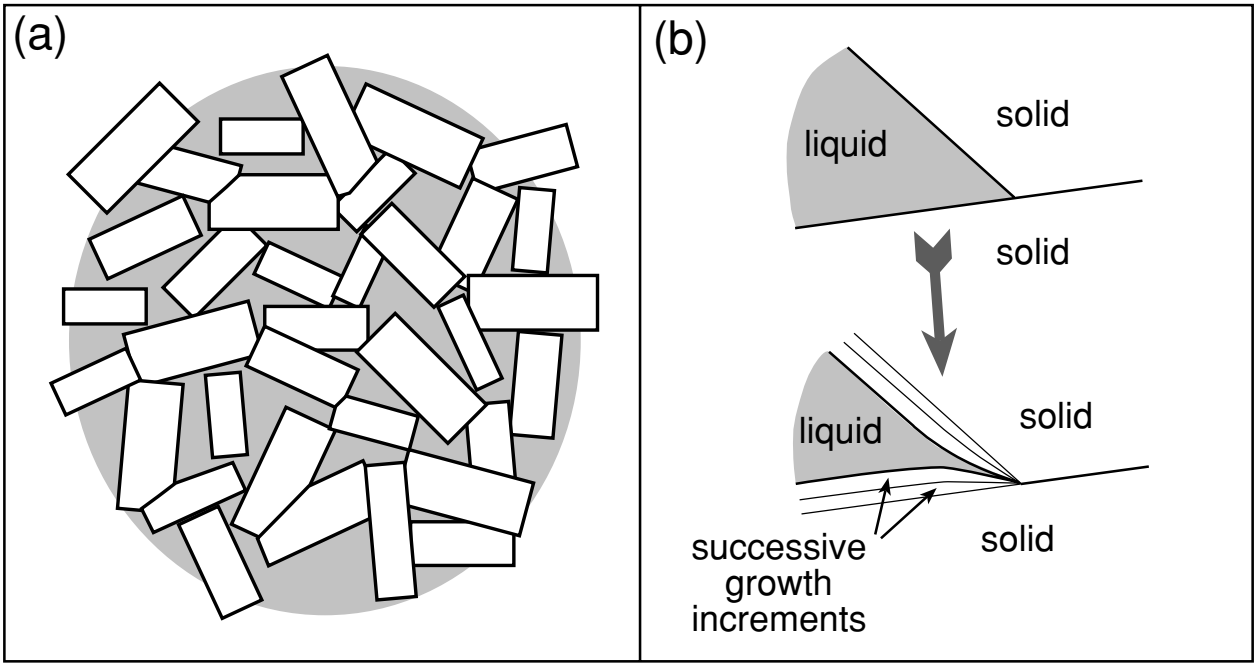

Figure 2. (a) The pore shape in a solidifying rock is determined by the juxtaposition of randomly positioned grains. Solid grains denoted by white, with the grey showing the porosity. (b) The modification of two-grain junctions by diffusion-limited growth. The compositional impoverishment of the liquid in the relatively confined region in the immediate vicinity of the two-grain junction means that growth in this region is inhibited, leading to a reduction in the angle subtended at the pore corner.

it is expected that crystal growth will occur faster than textural equilibration and so an impingement texture will form in the early stages of development of the crystal framework. Once growth has stopped, or slowed sufficiently, textural equilibration may occur, with adjustment of solid–melt surfaces at pore corners towards equilibrium (Holness, Cheadle & McKenzie, 2005). However, for magma emplaced into an open-system magma chamber, an additional control on the dihedral angle population is the timing of overturn and break-up of the replenishing layer. If crystallization-induced vesiculation in the replenishing magma reduces its density to that of the host while the replenishing layer is still much hotter than the latter, overturn and enclave formation will result in the sudden immersion of hot material in a cooler host. This will cause an episode of very rapid crystallization in the enclaves, manifest by overgrowth on the pre-existing grains.

The quench overgrowth will form protuberances or hopper-like forms and, given the probable change in pressure accompanying overturn, will have a composition discernibly different from that of the substrate. Experimental studies of textural evolution in amphibole- and biotite-melt aggregates shows that these overgrowths, formed during the quenching of the experimental run, can reduce the angle subtended at two-grain junctions (Laporte & Watson, 1995). This is because crystallization is so rapid that it becomes diffusion-limited. The relatively restricted region in the immediate vicinity of the two-grain junction becomes starved of chemical components necessary for crystal growth, and so growth can only progress some distance from the junction (Fig. 2b). This results in a change in curvature of the solid–melt interfaces and a reduction in the apparent angle. A preliminary study of the andesitic enclaves from the Kameni Islands, Santorini, showed that the angle reduction caused by quench-related growth can mimic progressive textural equilibration (Holness, Cheadle & McKenzie, 2005). Here we report a detailed investigation of the angle populations in the Kameni enclaves and show how it can be used to reveal information about the history of the open-system magma chamber.

3. Geological setting

Santorini is the largest volcanic centre in the Aegean Arc, formed by northwards subduction of the African plate beneath the continental Aegean microplate (e.g. Jackson, 1994). The islands of Palaea and Nea Kameni lie in the centre of the flooded Santorini caldera (Fig. 3a), for which the most recent activity was the Minoan eruption ~3600 years ago. The Kameni Islands are surrounded by the islands of Thera, Therasia and Aspronisi which preserve the remains of the pre-volcanic island and evidence for two cycles of explosive volcanic activity over the past 300 000 years (Druitt *et al*. 1989, 1999). The Kameni Islands have been the focus of historic intra-caldera volcanic activity on Santorini since the Minoan eruption, and now form a 2.5 km^3 intracaldera volcano, the summit of which rises ~500 m above the caldera floor (and ~100 m

https://doi.org/10.1017/S0016756805001172 Published online by Cambridge University Press

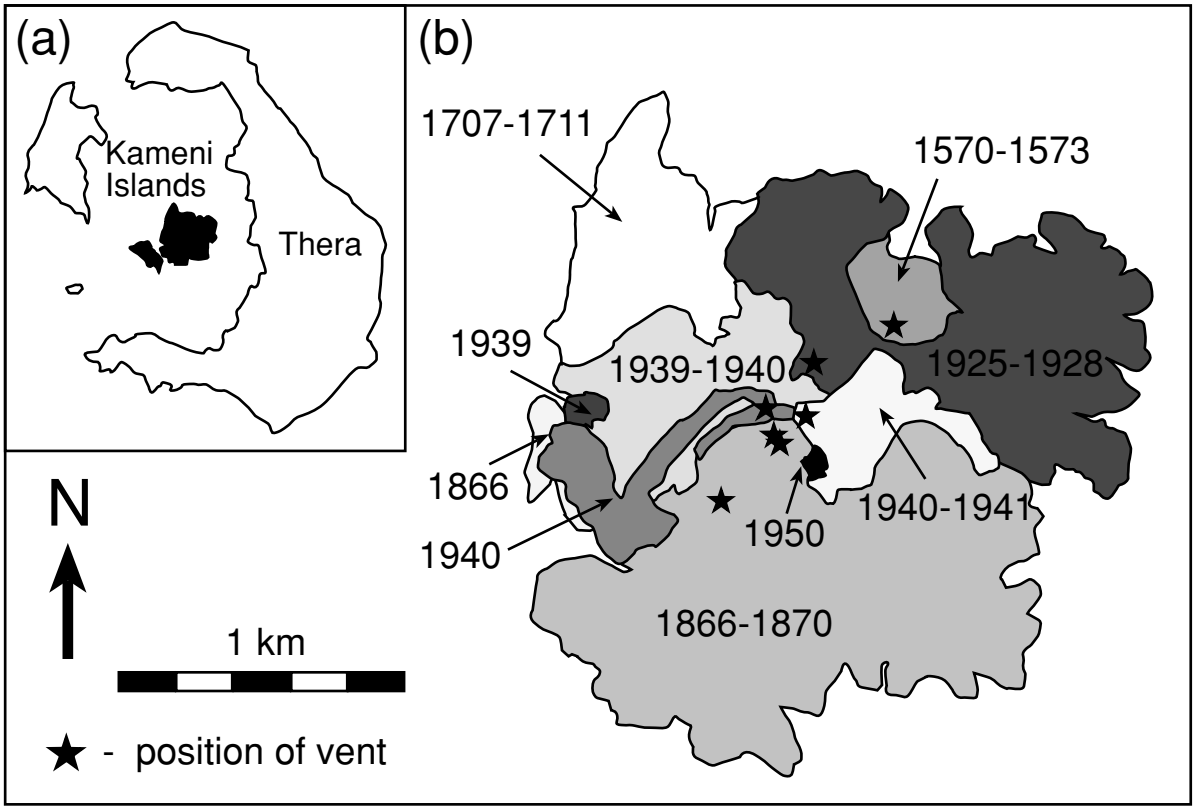

Figure 3. (a) Map showing the position of the Kameni Islands in the centre of the caldera formed by the outer islands of Thera. (b) Simplified map, after Druitt *et al*. (1999), showing the extent of the historical lava flows. We refer to the flow labelled 1570–1573 as the 1570 flow, that labelled 1939–1940 as the 1939 flow, that labelled 1940 as the 1940 flow, and that labelled 1940–1941 as the 1941 flow. The particular flows that were sampled for xenoliths were erupted from September 23, 1939 – July 9, 1940; July 12, 1940 – August 25, 1940; November 24, 1940 – early July 1941, and January 10 – February 2, 1950 (eruption dates from Georgalas, 1962).

above sea level: Huijsmans, 1985; Druitt *et al*. 1989, 1999). There have been at least nine sub-aerial episodes of volcanic activity since 197 BC, the last of which occurred in 1950 (Fig. 3b). The volume of magma erupted during each of these episodes is in the range $0.07–140 \times 10^6$ m^3 (data compiled by Higgins, 1996).

The islands are dacitic, and erupted compositions have remained approximately constant for the last ~2200 years, with whole rock SiO_2 contents varying from 64 to 68 wt % (Fig. 4; Huijsmans, 1985; Barton & Huijsmans, 1986). In detail, the lava compositions form two distinct groups, with earlier (pre-1866) flows having higher SiO_2 contents than later flows (Fig. 4). Detailed study of both the chemical compositions and the crystal size distribution of the plagioclase phenocrysts in the dacites of Kameni suggests that they result from the mixing of several different magmas (Barton & Huijsmans, 1986; Stamatelopoulou-Seymour *et al*. 1990; Higgins, 1996).

The near constancy of both the composition and the inferred temperature of the erupted dacite prompted Barton & Hiujsmans (1986) to postulate an essentially static history for the chamber over the last 2200 years. Consideration of crystal size distributions of plagioclase in the dacite led Higgins (1996) to refine this model to include successive periods of replenishment of the chamber with essentially aphyric dacite, which then mixed completely with the older, phenocryst-bearing host. He suggested that the subsequent eruption did not empty the chamber, leaving behind dacite into which further aphyric magma would later intrude. He used arguments based on plausible plagioclase growth rates to suggest that the aphyric magmas intruded into the magma chamber between 6 and 13 years prior to eruptions. These short timescales of storage and crystallization are consistent with observations of short-lived radioactive disequilibria in Kameni lavas, and with the patterns of zonation in Kameni phenocrysts (e.g. Druitt *et al*. 1999; Zellmer *et al*. 1999).

Recent investigations of the Kameni Islands have concentrated on the abundant magmatic enclaves, which are found in all the flows on the Kameni Islands, and which were first recognized by Fouqué (1879) and described in outline by Nicholls (1971). Using textural considerations the enclaves are interpreted to be quenched fragments of replenishing, relatively mafic magma (Martin, Holness & Pyle, 2005). Since the enclaves are more mafic than the host dacite lava, they formed from magma both hotter and denser than that occupying the chamber. From the absence of chilled margins to the enclaves, Martin, Holness & Pyle (2005) deduced that the replenishing magma

https://doi.org/10.1017/S0016756805001172 Published online by Cambridge University Press

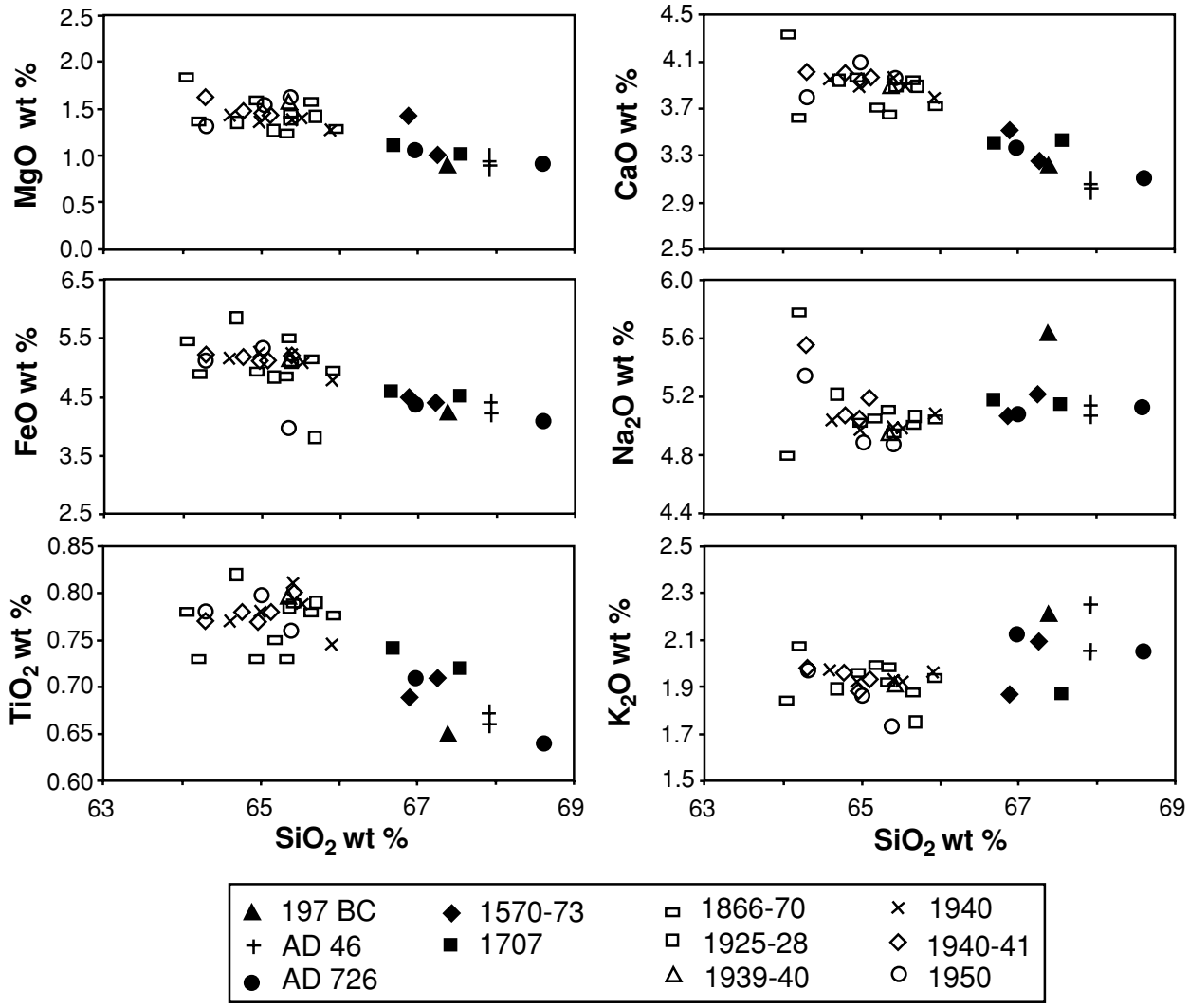

Figure 4. Representative bulk compositions of lavas from the Kameni Islands, differentiated according to the date of the flow. Note that flows pre-dating the 1866 eruption form a discrete group with slightly higher SiO_2 content than subsequent flows. Data from Huijsmans (1985), Francalanci *et al*. (1998), G. Zellmer, unpub. Ph.D. thesis, Open Univ., 1998 and this study.

initially formed a layer at the base of the chamber for each of the eruptions dating from 1570. This layer subsequently broke up and mixed with the host dacite once its bulk density had been sufficiently reduced by volatile exsolution, and was sampled during the subsequent eruption. Comparison of the composition of plagioclase phenocrysts in the dacite with that in the enclaves suggests that some of the phenocrysts were derived from the complete break-up of parts of this replenishing layer (Huijsmans, 1985; Martin, Holness & Pyle, 2005), although it is entirely plausible that the majority of them grew *in situ* in a large volume of dacite emplaced since 1850–1870 (Higgins, 1996).

Preliminary seismic data suggest that there is currently a region of shear wave attenuation consistent with the presence of partially molten material in a 4–5 km diameter region centred below the eastern margin of Nea Kameni at shallow depths (Delibasis *et al*. 1990). This is consistent with the conclusions of Barton & Huijsmans (1986), based on petrological arguments, that the current magma chamber is at a depth of 2–4 km. Given that the volume of each eruption forming the Kameni Islands (compiled by Higgins, 1996) represents only a small fraction of the likely total volume of a magma chamber of 4–5 km in diameter, it is clear that the historic eruptions did not result in complete emptying of the chamber.

The enclaves represent < 1 vol. % of the erupted material in each flow. Detailed study of grain-size relationships of the enclaves suggests that there is a positive correlation between the volume of each flow and the volume of replenishing magma (Martin, Holness & Pyle, 2005). Successive flows may contain very different enclave populations, with each flow typically containing a population dominated by a single enclave type, suggesting that each batch of replenishing magma may be almost entirely removed, either by eruption or by complete mingling consequent to break-up by expansion of volatiles, during the eruptive event which follows recharge (e.g. Martin, Holness & Pyle,

https://doi.org/10.1017/S0016756805001172 Published online by Cambridge University Press

Table 1. Representative bulk compositions for enclaves (each with a sample identification number), and host lavas

Sample	K8-186	K5-01	K4-02	K6-26	Lava compositions		
Date of flow	1570	1939–40	1940	1950	1570[1*]	1939[1]	1940[†]
SiO_2	60.06	56.84	57.66	55.65	67.26	65.38	65.45
TiO_2	1.11	1.21	1.13	1.24	0.71	0.79	0.80
Al_2O_3	16.53	16.66	16.53	16.52	15.27	15.56	15.68
Fe_2O_3	8.02	9.95	9.49	10.61	4.88	5.71	5.73
MnO	0.18	0.20	0.19	0.20	0.14	0.15	0.15
MgO	2.39	3.16	2.93	3.26	1.01	1.40	1.40
CaO	5.69	7.09	6.60	7.30	3.24	3.95	3.97
Na_2O	4.63	4.01	4.14	3.88	5.21	4.98	4.99
K_2O	1.28	0.99	1.15	0.96	2.1	1.9	1.92
Total	99.89	100.11	99.83	99.62	99.82	99.82	100.09
Ba	265	208	249	196	399	368	371
Cr	5	4	3	9	–	–	4
Ni	1	6	5	0	–	–	2
Nb	5.8	3.9	5.8	4.6	7.5	8.0	8.6
Rb	41	26	37	27	69.3	65.3	63
Sr	221	228	219	232	145	163	159
Sc	18	27	22	28	–	–	17
V	103	275	229	307	–	–	56
Y	36.9	36.1	36.2	33.9	–	–	44.6
Zr	152	121	136	116	–	–	217

The major elements are given as weight %, and traces as ppm. Data from G. Zellmer, unpub. Ph.D. thesis, Open Univ., 1998 denoted by [1]. The composition of the 1570 lava used for the MELTS calculations is denoted *, and that of the 1940 lava is denoted [†]. The composition of enclave K6–26 was used to derive Figure 9.

2005). Alternatively, relicts of the intruding layer may solidify completely and not be sampled by subsequent eruptions.

The present study is concerned with andesitic enclaves which dominate the enclave population in the 1939, 1940 and 1950 flows (the A1 type of Martin, Holness & Pyle, 2005). Significant numbers of a texturally identical type of enclave are also present in the 1570 flow. The enclave population in the 1941 flow is dominantly basaltic, but rare A1-type enclaves are also present. Martin, Holness & Pyle (2005) suggest that these rare A1 enclaves are remnants of replenishing material from the 1940 eruption, which stopped three months earlier.

The A1-type enclaves form ellipsoidal to spherical blocks up to 60 cm long, and have an andesitic bulk composition which is essentially identical for those enclaves from the 1939, 1940, 1941 and 1950 flows, although slightly more SiO_2-rich in the 1570 flow (Table 1). They comprise a crystalline mass dominated by plagioclase, with subsidiary amounts of clinopyroxene, orthopyroxene and titanomagnetite. The interstitial material comprises fresh glass and vesicles, with the latter occupying up to 25 vol. % of the bulk. The grain-size population of the plagioclase (reproduced from Martin, Holness & Pyle, 2005, as Fig. 5) gives a straight crystal size distribution (CSD), characteristic of a single population of plagioclase grains. Additionally, the CSDs of the A1 enclaves in the five flows are similar, attesting to similar growth conditions for each (Martin, Holness & Pyle, 2005; Fig. 5).

Given the constant slope of the CSD, we interpret A1 enclaves to have formed by quenching of an aphyric andesitic melt which was injected as a layer at the base of the shallow magma chamber. The aphyric nature of this relatively evolved liquid was most likely the result of filter-pressing of a fractionating magma deeper in the plumbing system. Eruption of the enclave-bearing flow may have occurred in response to a positive feedback process involving expansion of the exsolved gas during upwards movement of the replenishing layer once it had crystallized sufficiently to attain neutral buoyancy. While there is no contemporary record of local seismicity, or other observations, that might relate to the timing of any pre-eruptive replenishment event, a lower bound on the crystallization timescale is provided by the complete change in enclave population between the 1940 and 1941 flows (apart from the rare A1-type enclaves in the latter), suggesting that the magma forming the basaltic enclaves dominating the 1941 flow may have entered the chamber only three months before eruption (Martin, Holness & Pyle, 2005).

If we assume that all the crystalline material in the A1 enclaves formed in the shallowest magma reservoir, this means that the preserved textures record only crystallization events and textural adjustment immediately prior to eruption of the entraining dacite. It is significant that the grain size distribution of the A1-type enclaves is constant, regardless of the flow in which they are found (Fig. 5), demonstrating that each experienced essentially the same nucleation and growth rates, controlled, presumably, both by the size of the replenishing magma batch, and by the thermal and compositional contrast between the replenishing magma and the host (e.g. Bacon, 1986; Martin, Holness & Pyle, 2005). The presence of A1-type enclaves in five separate flows in Nea Kameni, together with the near

https://doi.org/10.1017/S0016756805001172 Published online by Cambridge University Press

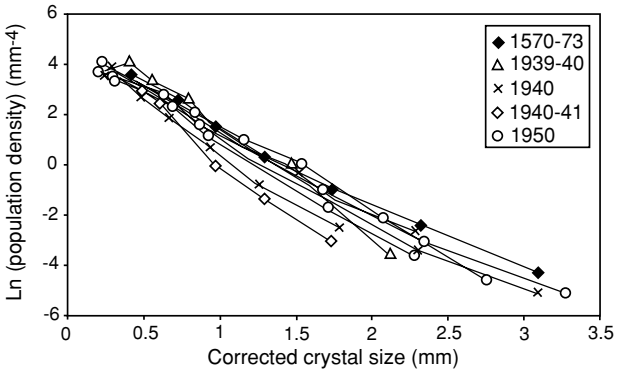

Figure 5. Crystal Size Distribution (CSD) for plagioclase populations in a representative suite of A1 type enclaves. Note the straight line plot for each, demonstrating that the plagioclase crystals were derived from a single growth episode, and do not contain an older population of phenocrysts. From Martin, Holness & Pyle (2005).

constancy of both enclave and host dacite composition and macro-scale textures in the enclaves, provides an ideal suite of samples in which to examine the variation of dihedral angle populations.

4. Analytical techniques

Following the metallurgists, who pioneered work in the field using opaque materials, geologists have generally measured dihedral angles using a conventional microscope stage or by analysis of images generated by electron microscopy. This method relies on measuring a population of angles on a randomly oriented two-dimensional section through the material. For samples containing a single true value of dihedral angle it can be shown that the median of a population of these angles is within 1° of the true three-dimensional angle (Riegger & Van Vlack, 1960; Harker & Parker, 1945). For other samples, including most of geological interest, sophisticated statistical techniques are required to constrain the range of true equilibrium angles (e.g. Jurewicz & Jurewicz, 1986).

Given the significance of information contained within the actual population of true three-dimensional angles, we used a universal stage mounted on an optical microscope to measure true 3-D dihedral angles. We used a binocular Leitz-Wetzlar Ortholux optical microscope fitted with a Leitz-Wetzlar 4-axis Universal Stage, permitting rotation of the thin-section by up to 90° in the vertical direction. Measurements of 60 to 80 true 3-D dihedral angles were obtained from each of 22 samples. For six of the 22 samples, the angle between the planar growth faces far from the grain junctions was also measured. The accuracy of each measurement is of the order of a few degrees.

Plagioclase quench growth consequent to layer overturn is visible optically as an outer zone of different birefringence, with a sharply defined boundary with the substrate. The width of this quench growth on the long faces of the plagioclase crystals was measured using a Zeiss micrometer, with an accuracy of individual measurements of < 1 μm at a magnification of $\times$ 400, mounted on an optical microscope with a flat stage. Only well-defined zones were measured, to minimize the effects of random intersections through the crystals. Measurements were made in regions of uniform thickness, avoiding two-grain junctions. Up to 30 individual measurements were made in each sample. The standard deviations for each of the populations was in the region of 4–8 μm.

Whole rock major and trace element analyses were performed at the Open University on an ARL wavelength-dispersive XRF spectrometer, using standard techniques described in Ramsey *et al*. (1995). The major element compositions of plagioclase were obtained using a Cameca SX-100 electron microprobe at the University of Cambridge. Mineral analyses were conducted using a 5 μm beam diameter, a 15 keV accelerating voltage and a beam current of 10 nA.

5. Textural observations

The A1-type enclaves from each of the five flows have a solid fraction dominated by blocky crystals of plagioclase with no preferred orientation (Fig. 6a, b). This is the dominant framework-forming phase. Devolatilization of the final liquid was almost complete during emplacement and eruption, based on high totals for electron microprobe analyses (V. M. Martin, unpub. data). Given the large molar volume of H_2O at the high temperatures and low pressures ($\sim$ 1 bar) at the vent, we believe that most of the exsolved H_2O escaped from the enclaves, either along large channels in the crystal framework or by rapid expulsion along the fractures within the layer which now form the boundaries of the enclaves. The remaining 25–30 vol. % void fraction represents the maximum amount that can be contained in the crystal framework.

The framework-forming plagioclase crystals are commonly normally zoned, with no oscillatory zoning. This probably indicates growth *in situ* from a static melt phase in which the volatiles could exsolve in a continuous manner (J. D. Blundy, pers. comm. 2004). The crystals commonly have elongate extensions indicative of a period of rapid crystallization (Fig. 6b). These extensions are associated with a well-defined marginal region, which has a different birefringence to the substrate (Fig. 6b–d). This is a consequence of the generally more albitic composition of the outer zone (Ab_{40-80}) compared with that of the central parts of the grains (Ab_{29-50}). Most plagioclase grains are isolated, while others form small clumps with subsidiary crystals nucleating on, and growing at high angles away from, the larger host (Fig. 6a, c).

In the vicinity (within a few tens of micrometres) of the junctions between two grains, the otherwise planar

https://doi.org/10.1017/S0016756805001172 Published online by Cambridge University Press

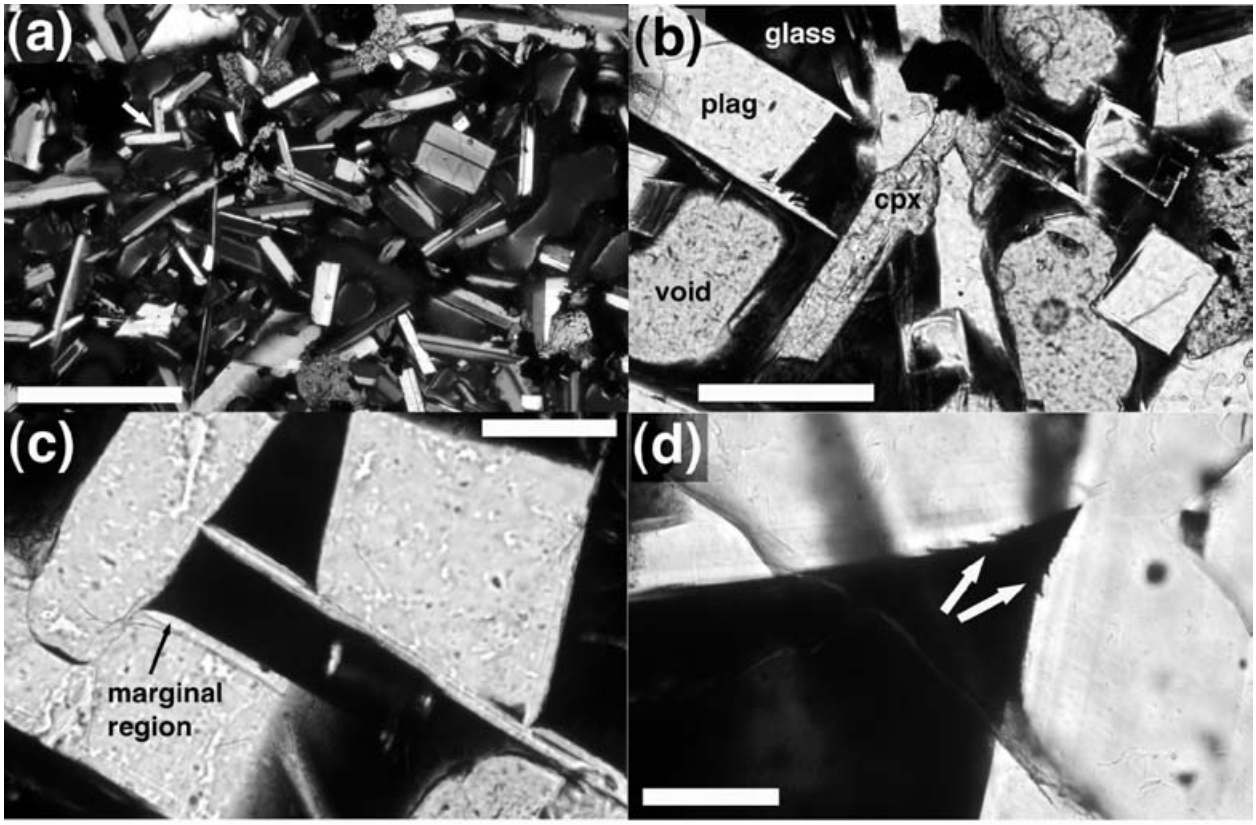

Figure 6. Photomicrographs of A1-type enclaves from the Kameni Islands. (a) Plagioclase forms the framework, with minor amounts of clinopyroxene (irregular grains). The interstitial material is glass (black) with abundant vesicles. The arrow shows a pair of grains joined at high angle, possibly due to heterogeneous nucleation. Crossed polars, scale bar 1 mm long. (b) Plagioclase grains have elongate extensions which are associated with the marginal region of slightly more albitic composition. This image shows several grains intersected in the region of the extensions, and they appear as totally skeletal forms. Scale bar is 200 μm long. (c) Plagioclase grains (white) commonly form glomerocrysts with grains juxtaposed at high angles, presumably due to lattice orientation control on nucleation sites. At the pore corners, the initial impingement angles are being replaced by lower angles during quenching. Note the well-defined albitic marginal region, which coincides with the tip of the re-entrants at two-grain junctions. The matrix is dark glass. Plane polarized light. Scale bar is 200 μm long. (d) The angle between two adjacent plagioclase grains has been narrowed during diffusion-limited growth caused by quenching. Note how the plagioclase surfaces in the region intermediate between the smooth planar growth facets and the equilibrated region are irregular (arrowed), suggestive of breakdown of the otherwise planar growth faces due to rapid, diffusion-limited, crystallization. Plane polarized light. Scale bar 100 μm long.

growth faces develop curvature into the pore corner (Fig. 6c, d). These curved areas may end in a region with an irregular surface (Fig. 6d), reminiscent of the larger-scale hopper-like growth extensions (Fig. 6b). These curved regions are developed entirely within the outermost zone, and they are largest, and best developed, in samples with wide marginal zones on the plagioclase.

The populations of dihedral angles subtended at two-grain junctions differ between flows (Fig. 7). While the median dihedral angles, and the standard deviation from the mean, of all enclaves from each flow form a tight cluster (Fig. 7b), each of the five flows has a characteristic signature. For comparison, the impingement angles formed by the juxtaposition of adjacent growing grains, measured from six different samples, are also shown. The signature of an impingement texture in plagioclase crystal frameworks is one of high dihedral angle (58–62°) with a high standard deviation (25–35°). The population of actual angles form a trend away from these unmodified impingement populations towards that of a texturally equilibrated aggregate (from Holness, Cheadle & McKenzie, 2005).

The width of the quench-related overgrowth also shows differences between the flows. Measurements of overgrowth width in ten samples (chosen to cover the full range of median dihedral angles) demonstrates a strong negative correlation between average thickness and the median dihedral angle (Fig. 8). Thus the thicker rims are associated with the lowest dihedral angles.

6. Interpretation of textural observations

The cluster of data points showing the median and standard deviation of populations of apparent angles formed by impingement forms a trend towards a median of 90° at zero standard deviation (shown by the grey arrow on Fig. 7b). We suggest that this trend may be

https://doi.org/10.1017/S0016756805001172 Published online by Cambridge University Press

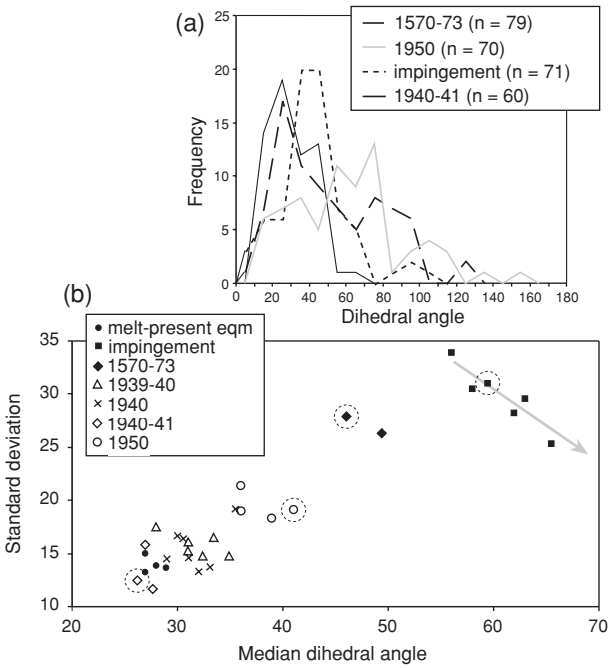

Figure 7. Dihedral angle population data for A1-type enclaves in the Kameni Islands. (a) Frequency plots for observed dihedral angle for representative samples covering the entire range of angle populations. The number of observations for each sample is given by *n*. (b) Median plagioclase–plagioclase–glass dihedral angle plotted against the population standard deviation. The circled points denote samples shown in Figure 7a. The impingement data were obtained from measuring angles between adjacent grains, far from the grain boundary. The grey arrow shows the trend towards a median of 90° and a zero standard deviation, corresponding to a texture in which all plagioclase–plagioclase junctions are at 90°, perhaps promoted by heterogeneous nucleation with a preferred crystallographic orientation relative to the host grain. The equilibrium data are from Holness, Cheadle & McKenzie (2005).

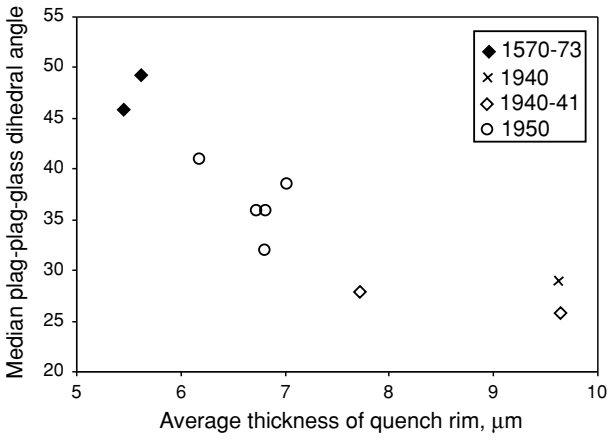

Figure 8. The average width of the quench-related albitic rims on the plagioclase grains compared with the median plagioclase–plagioclase–glass dihedral angle.

the result of heterogeneous nucleation of plagioclase on existing plagioclase grains.

The first work on textures in fluid-bearing rocks generated only by crystal growth was that of Elliot, Cheadle & Jerram (1997) who developed computer simulations of polycrystalline solidifying liquids. They investigated apparent dihedral angle populations generated by randomly oriented grains of differing shape, ranging from spheres to cubes and laths. For closed pores, the median of the population of apparent dihedral angles is 60°, since the three internal angles of a triangle sum to 180°. A median angle of 90° occurs for cubic and lath-like grain shapes forming open pores (that is, junctions between only two grains) (Elliot, Cheadle & Jerram, 1997).

Although the impingement texture populations determined for the Kameni enclaves form a trend towards a median of 90°, we believe this trend is not a result of mixing one distribution characterized by closed pores with another characterized by randomly oriented grains in a texture dominated by open pores. The reason for this is because the trend we observe is towards a zero standard deviation, rather than the high standard deviation we would expect for random orientation (although Elliot, Cheadle & Jerram, 1997, did not calculate standard deviations). It is thus a trend towards a texture dominated by plagioclase grains impinging at 90°, which is most plausibly the result of heterogeneous nucleation of plagioclase. This suggests that crystals preferably nucleate on pre-existing plagioclase grains with the long axes of the two grains perpendicular to each other. This is apparent in Figure 6a and c.

The statistical significance of the differences between enclaves derived from different flows was examined using non-parametric statistical methods. The Mann-Whitney 'U' test (which is used to compare the medians of two data sets randomly sampling populations of unknown form to constrain the likelihood that the underlying populations are the same: Siegel, 1956) demonstrates that the differences in median and standard deviation of dihedral angles measured in different enclaves from the same flow are not significant. Similarly, the populations of dihedral angles measured in enclaves from the group of flows dating from 1939 to 1941 are not significantly different, although there is a marginal significance in the difference between the enclaves from the 1941 flow and the enclave with the highest median angle of the 1939 cluster. However, the angles in the enclaves from this set of flows and those from the 1950 group and the 1570 group form statistically distinct populations.

The relationship between the width of the quench overgrowths and the median value of the dihedral angle population (Fig. 8), together with the observation that the re-entrants at two-grain junctions occur entirely within the quench overgrowths, is consistent with the modification of the original impingement populations being a consequence of quench overgrowth (e.g. Laporte & Watson, 1995). That the trend away from impingement is indistinguishable from that of progressive textural equilibration (Holness, Cheadle & McKenzie, 2005) is simply an artifact related to the fact

https://doi.org/10.1017/S0016756805001172 Published online by Cambridge University Press

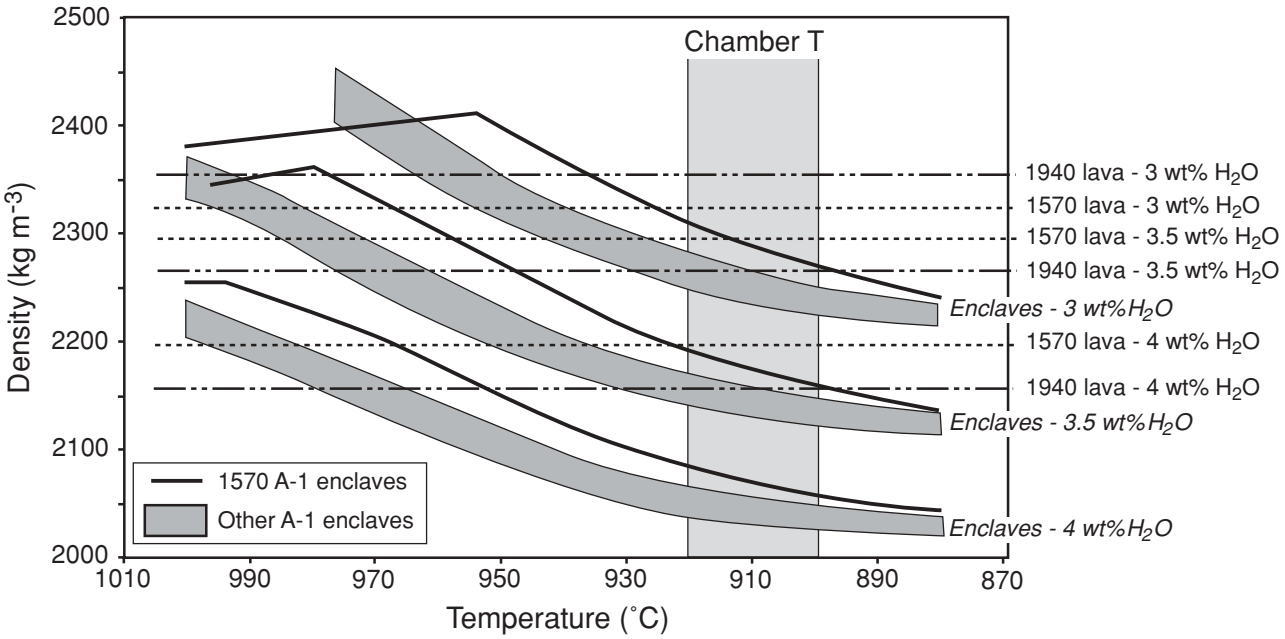

Figure 9. The changing bulk density of the layer of replenishing magma, as a function of H_2O content, during cooling-driven crystallization, given by dark shaded bands (for the range of bulk compositions of A1-type enclaves from the 1939–1941 set of flows, see Table 1) or heavy lines (for the A1-type enclaves in the 1570 flow, see Table 1). The temperature of the host dacite is shown by the shaded box, together with calculated densities of the host dacite as a function of H_2O content for both a typical dacite composition from the 1939–1941 flows (see Table 1) and a typical composition for the 1570 flow (Table 1). The calculations were carried out assuming no loss of H_2O during crystallization. See text for details.

that both the quench-modified trend and progressive equilibration trend need to pass through the origin. Hence, the enclaves with the lowest dihedral angles are those in which the greatest amount of crystallization occurred during the phase of rapid crystal growth consequent to layer overturn.

7. Controls on overturn and eruption

As a simple model, we postulate that crystallization in the replenishing layer at the base of the chamber causes the bulk density of the replenishing layer to decrease to that of the host dacite, triggering overturn and eruption. The variation in dihedral angle populations between flows is then a function of the variation in temperature difference between the overturning layer and the resident dacite for each of the eruptions. Given the similarity of major element compositions for the enclaves and host dacite, what is the factor which resulted in these differences?

We investigated the variation of bulk density with temperature using the program MELTS (Ghiorso & Sack, 1995; Asimow & Ghiorso, 1998). The composition of the 1939–1941 dacitic flows is uniform (a typical bulk composition is given in Table 1). The dacite from the 1570 flow was taken to be an average of the available analyses (Table 1). Using these compositions, we calculated the density of the host dacite at the estimated chamber temperature of 900–920 °C (Huijsmans, 1985; Barton & Huijsmans, 1986) using a range of plausible H_2O contents of 3–4 wt % (Huijsmans, 1985; Barton & Huijsmans, 1986) and at pressures of 1–2 kbar. For pressures > 1.5 kbar, crystallization of the replenishing magma does not reduce the bulk density to values lower than that of the host dacite before thermal equilibration occurs. This scenario would result in stable stratification of the chamber and no overturn. For pressures < 0.5 kbar, the bulk density of the replenishing magma is typically lower than that of the host dacite on injection. For this reason we confined our modelling to a pressure of 1 kbar, consistent with the observations of microseismicity at depths of ~ 5 km (Delibasis *et al*. 1990), and the geobarometric estimates of Barton & Huijsmans (1986). Figure 9 shows the change in bulk density during crystallization of the replenishing andesite for a range of plausible H_2O contents at 1 kbar, compared with that of the resident dacite.

For a given host dacite H_2O content, the bulk density of the intruding layer reaches that of the host dacite magma at successively lower temperatures as the H_2O content of the replenishing magma is decreased. If the bulk density of the replenishing layer is higher than that of the dacite when the temperature of the replenishing layer reaches that of the dacite, the layer will be gravitationally stable. This means that overturn, and consequent eruption, will not occur. If, on the other hand, the bulk density of the replenishing layer reaches that of the dacite before the temperature of the replenishing layer reaches that of the dacite, there

https://doi.org/10.1017/S0016756805001172 Published online by Cambridge University Press

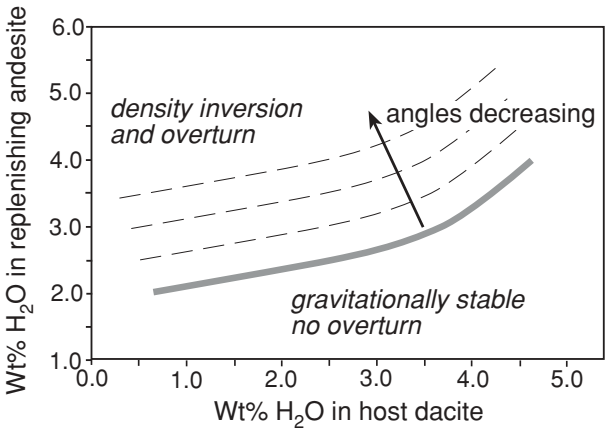

Figure 10. Sketch showing the relationship between host dacite and replenishing magma H_2O content and the relative timing of attainment of thermal equilibrium and neutral buoyancy. For systems lying below the heavy grey line, the replenishing layer is still denser than the dacite when it has cooled to the same temperature; for such systems there will be no overturn. For systems lying above the line, the replenishing magma will become less dense than the dacite while it is still hotter than the resident magma. These systems will overturn. The further the system is above the grey line, the lower the resultant quench-modified dihedral angles will be. The calculations were carried out at 1 kbar, using an average enclave composition and an average dacite composition from the 1940 flow.

will be overturn. The amount of quench-related growth, and modification of the original impingement angle population, will be a function of the temperature difference between the overturning layer and the dacite. For example, in a chamber containing dacite with 3 wt % H_2O, the overturn of a replenishing magma containing 3.5 wt % H_2O will occur at temperatures $\sim 50\,^{\circ}C$ higher than for a replenishing magma containing 3 wt % H_2O. Figure 9 shows that, for a given dacite H_2O content, the greatest amount of modification of the impingement texture, and reduction of the median dihedral angle, will occur for the wettest replenishing magma.

There is a critical division between a stably stratified chamber and an overturning chamber at the point where neutral buoyancy occurs at the temperature of the dacite. We have calculated this line at a pressure of 1 kbar, using an average enclave composition and an average dacite composition from the 1940 flow (Fig. 10). If the initial dissolved H_2O content of the replenishing magma lies above this line, the replenishing chamber will be unstable and will overturn for any given host dacite H_2O content. Additionally, for a given dacite H_2O content, the median of the dihedral angle population in the enclaves will decrease as the water content of the replenishing magma is increased. For those below the line, the chamber will not overturn.

Although the major element compositions of the 1570 lava and A1-type enclaves in the 1570 lava differ slightly from the other flows (Fig. 4, Table 1), the effect of changing composition is not as significant as that of changing the H_2O content of either magma. Since the major element compositions of both host dacite and A1-type enclaves in the 1950 flow are indistinguishable from the 1939–1941 flows and enclaves, the only variable which may account for the statistically significant difference in the extent of textural equilibration of the plagioclase–plagioclase–melt dihedral angles between the 1939–1941 and the 1950 flows is the H_2O content of either the host dacite or the replenishing magma. The high dihedral angles in the enclaves from the 1570 eruption demonstrate that the H_2O contents of both the replenishing magma and the resident dacite lay close to the critical dividing line in Figure 10.

The similarity of the enclaves in the 1939, 1940 and 1941 flows suggests that for a given host dacite H_2O content (which is unlikely to change significantly on this timescale) the replenishing magma had a constant H_2O content. If the host dacite H_2O content remained constant until 1950, the differences in dihedral angle population in the 1950 enclaves are consistent with this eruption being due to the replenishment of the chamber by a magma with a slightly lower H_2O content than that responsible for the 1939–1941 eruptions.

Given the similarity of the 1939–1941 eruptions, could they have been the result of a single replenishment event? The grain size distribution of the plagioclase crystals in each set of enclaves is indistinguishable (Fig. 5), so there is no signature of an increased grain growth in the later eruptions. The dihedral angle populations in the enclaves from the three flows are also similar, although the lowest dihedral angles are seen in the enclaves from the 1941 flow. However, this particular flow is dominated by basaltic enclaves, with only very rare A1-type enclaves. We suggest, following Martin, Holness & Pyle (2005), that the eruptions of 1939 and 1940 were triggered by two separate injections of identical andesitic magma, whereas the 1941 eruption was triggered by a basaltic replenishment. The rare A1 enclaves in the 1941 flow represent small amounts of the earlier material dating from the previous replenishment. The lower dihedral angles, and greater amount of quench-related growth, in these samples are most probably the result of a greater temperature difference caused by the re-heating of the small amounts of remaining andesite by the incoming basaltic material. The corollary of this is that plagioclase grain growth was not sufficient to alter the CSD significantly on this time scale.

8. Conclusions

We have shown that there is a wealth of information encoded in the textures developed in the crystal mush forming in layers of replenishing magma at the base of an open-system chamber. Detailed observations and measurement of the angle between adjacent grains of a framework-forming phase provide valuable information on the dynamics of magma chamber

https://doi.org/10.1017/S0016756805001172 Published online by Cambridge University Press

replenishment and eruption. In particular, our data are consistent with pinpointing the importance of magma H_2O content in controlling eruption dynamics. The overturn of a wet replenishing magma occurs while the layer is hotter than an otherwise identical magma with a lower H_2O content. While this can be predicted using currently available models of magmatic evolution, our work shows that the textures of enclaves record these differences.

Acknowledgements. This work was carried out during the tenure of a NERC post-graduate studentship number NER/S/2001/05965 (VM). The work was supported in part by the European Community's Human Potential Programme under contract HPRN-CT-2002–000211 (EUROMELT), and by Queens' College, Cambridge and the Cambridge Philosophical Society. We thank IGME, Athens, for permission to carry out fieldwork and collect samples, R. Walker and N. Ireland for assistance in the field, and S. T. C. Siklos for helpful discussions. Thoughtful and helpful comments from Michael Higgins, Alexander Mock and an anonymous reviewer greatly improved an earlier version of the manuscript.

References

ASIMOW, P. D. & GHIORSO, M. S. 1998. Algorithmic modifications extending MELTS to calculate subsolidus phase relations. *American Mineralogist* **83**, 1127–31.

BACON, C. R. 1986. Magmatic inclusions in silicic and intermediate volcanic rocks. *Journal of Geophysical Research* **91**, 6091–112.

BACON, C. R. & METZ, J. 1984. Magmatic inclusions in rhyolites, contaminated basalts and compositional zonation beneath the Coso volcanic field, California. *Contributions to Mineralogy and Petrology* **85**, 346–65.

BARTON, M. & HUIJSMANS, J. P. P. 1986. Post-caldera dacites from the Santorini volcanic complex, Aegean Sea, Greece: an example of the eruption of lavas of near-constant composition over a 2200 year period. *Contributions to Mineralogy and Petrology* **94**, 472–95.

BLUNDY, J. & CASHMAN, K. 2001. Ascent-driven crystallization of dacite magmas at Mount St Helens, 1980–1986. *Contributions to Mineralogy and Petrology* **140**, 631–50.

CAMPBELL, I. H. 1996. Fluid dynamic processes in basaltic magma chambers. In *Layered intrusions* (ed. R. G. Cawthorn), pp. 45–76. Amstersdam: Elsevier Science.

COOMBS, M. L., EICHELBERGER, J. C. & RUTHERFORD, M. J. 2002. Experimental and textural constraints on mafic enclave formation in volcanic rocks. *Journal of Volcanology and Geothermal Research* **119**, 125–44.

COUCH, S., SPARKS, R. S. J. & CARROLL, M. R. 2001. Mineral disequilibrium in lavas explained by convective self-mixing in open magma chambers. *Nature* **411**, 1037–9.

DELIBASIS, N., CHAILAS, S., LAGIOS, E. & DRAKOPOULOS, D. 1990. Surveillance of Thera Volcano, Greece: microseismicity monitoring. In *Thera and the Aegean World III, 2* (ed. D. A. Hardy), pp. 199–206. London: The Thera Foundation.

DRUITT, T. H., EDWARDS, L., MELLORS, R. M., PYLE, D. M., SPARKS, R. S. J., LANPHERE, M., DAVIES, M. & BARREIRO, B. 1999. *Santorini Volcano*. Geological Society of London, Memoir no. 19.

DRUITT, T. H., MELLORS, R. M., PYLE, D. M. & SPARKS, R. S. J. 1989. Explosive volcanism on Santorini, Greece. *Geological Magazine* **126**, 95–126.

EICHELBERGER, J. C. 1995. Silicic volcanism: ascent of viscous magmas from crustal reservoirs. *Annual Review of Earth and Planetary Science* **23**, 41–63.

ELLIOTT, M. T., CHEADLE, M. J. & JERRAM, D. A. 1997. On the identification of textural equilibrium in rocks using dihedral angle measurements. *Geology* **25**, 355–8.

FAUL, U. H. 1997. Permeability of partially molten upper mantle rocks from experiments and percolation theory. *Journal of Geophysical Research* **102**, 10299–311.

FOUQUÉ, F.1879..*Santorin et ses éruptions*. Paris: Masson et cie, pp. 1–440.

FRANCALANCI, L., VOUGIOUKALAKIS, G., ELEFTHERIADES, G., PINARELLI, L., PETRONE, C., MANETTI, P. & CHRISTOFIDES, G. 1998. Petrographic, chemical and isotopic variations in the intra-caldera post-Minoan rocks of the Santorini volcanic field, Greece. In *Proceedings of the second workshop, Santorini, Greece, 2 to 4 May 1996* (eds R. Casale, M. Fytikas, G. Sigvaldasson and G. Vougioukalakis), pp. 175–86. Brussels: European Commission.

GEORGALAS, G. C. 1962. *Catalogue of the Active Volcanoes of the World including Solfatara Fields, Greece.* International Association of Volcanology, Rome.

GHIORSO, M. S. & SACK, R. O. 1995. Chemical mass transfer in magmatic processes. IV. A revised and internally consistent thermodynamic model for the interpolation and extrapolation of liquid–solid equilibria in magmatic systems at elevated temperatures and pressures. *Contributions to Mineralogy and Petrology* **119**, 197–212.

HARKER, D. & PARKER, E. R. 1945. Grain shape and grain growth. *Transactions of the American Society of Metals* **34**, 156–95.

HAWKESWORTH, C., GEORGE, R., TURNER, S. & ZELLMER, G. 2004. Time scales of magmatic processes. *Earth and Planetary Science Letters* **218**, 1–16.

HIGGINS, M. D. 1996. Magma dynamics beneath Kameni Volcano, Thera, Greece, as revealed by crystal size and shape measurements. *Journal of Volcanology and Geothermal Research* **70**, 37–48.

HOLNESS, M. B., CHEADLE, M. J. & MCKENZIE, D. 2005. On the use of dihedral angle change to decode late-stage textural evolution in cumulates. *Journal of Petrology* **46**, 1565–83.

HUIJSMANS, J. P. P. 1985. Calcalkaline lavas from the volcanic complex of Santorini, Aegean Sea, Greece. *Geologica Ultraiectina* **41**, 1–316.

HUPPERT, H. E. & SPARKS, R. S. J. 1980. The fluid dynamics of a basaltic magma chamber replenished by influx of hot, dense, ultrabasic magma. *Contributions to Mineralogy and Petrology* **75**, 279–89.

HUPPERT, H. E., TURNER, J. S. & SPARKS, R. S. J. 1982. Replenished magma chambers: effects of compositional zonation and input rates. *Earth and Planetary Science Letters* **57**, 345–57.

JACKSON, J. A. 1994. Active tectonics of the Aegean region. *Annual Reviews of Earth and Planetary Sciences* **22**, 239–71.

JAMTVEIT, B. & ANDERSEN, T. B. 1992. Morphological instabilities during rapid growth of metamorphic garnets. *Physics and Chemistry of Minerals* **19**, 176–84.

JUREWICZ, S. R. & JUREWICZ, A. J. G. 1986. Distribution of apparent angles on random sections, with emphasis on

dihedral angle measurements. *Journal of Geophysical Research* **91**, 9277–82.

LAPORTE, D. 1994. Wetting behaviour of partial melts during crustal anatexis: the distribution of hydrous silicic melts in polycrystalline aggregates of quartz. *Contributions to Mineralogy and Petrology* **116**, 486–99.

LAPORTE, D. & WATSON, E. B. 1995. Experimental and theoretical constraints on melt distribution in crustal sources – the effect of crystalline anisotropy on melt interconnectivity. *Chemical Geology* **124**, 161–84.

LOFGREN, G. E. 1974. An experimental study of plagioclase crystal morphology: isothermal crystallization. *American Journal of Science* **274**, 243–73.

MARTIN, V. M., HOLNESS, M. B. & PYLE, D. M. 2005. Textural analysis of magmatic enclaves from the Kameni Islands, Santorini, Greece. *Journal of Volcanological and Geothermal Research*, in press.

MURPHY, M. D., SPARKS, R. S. J., BARCLAY, J., CARROLL, M. R. & BREWER, T. S. 2000. Remobilisation of andesite magma by intrusion of mafic magma at the Soufriere Hills Volcano, Montserrat, West Indies. *Journal of Petrology* **41**, 21–42.

NICHOLLS, I. A. 1971. Petrology of Santorini volcanic rocks. *Journal of Petrology* **12**, 67–119.

PALLISTER, J. S., HOBLITT, R. P. & REYES, A. G. 1992. A basalt trigger for the 1991 eruptions of Pinatubo Volcano. *Nature* **356**, 426–8.

PHILLIPS, J. C. & WOODS, A. W.2002. Suppression of large scale magma mixing by melt–volatile separation. *Earth and Planetary Science Letters* **204**, 47–60.

PHILPOTTS, A. R., BRUSTMAN, C. M., SHI, J. Y., CARLSON, W. D. & DENISON, C. 1999. Plagioclase-chain networks in slowly cooled basaltic magma. *American Mineralogist* **84**, 1819–29.

RAMSEY, M. H., POTTS, P. J., WEBB, P. C., WATKINS, P., WATSON, J. S. & COLES, B. J. 1995. An objective assessment of analytical method precision: comparison of ICP-AES and XRF for the analysis of silicate rocks. *Chemical Geology* **124**, 1–19.

REAGAN, M. K., SIMS, K. W. W., ERICH, J., THOMAS, R. B., CHENG, H., EDWARDS, R. L., LAYNE, G. & BALL, L. 2003. Time-scales of differentiation from mafic parents to rhyolite in North American continental arcs. *Journal of Petrology* **44**, 1703–26.

RIEGGER, O. K. & VAN VLACK, L. H. W. 1960. Dihedral angle measurement. *Transactions of the Metallurgical Society of the AIME* **218**, 933–5.

SIEGEL, S. 1956. *Nonparametric statistics for the behavioural sciences.* New York: McGraw-Hill.

SNYDER, D. & TAIT, S. 1995. Replenishment of magma chambers: comparison of fluid-mechanic experiments with field relations. *Contributions to Mineralogy and Petrology* **122**, 230–40.

SNYDER, D. & TAIT, S. 1996. Magma mixing by convective entrainment. *Nature* **379**, 529–31.

SPARKS, R. S. J. & MARSHALL, L. A. 1986. Thermal and mechanical constraints on mixing between mafic and silicic magmas. *Journal of Volcanology and Geothermal Research* **29**, 99–124.

SPARKS, R. S. J., SIGURDSSON, H. & WILSON, L. 1977. Magma mixing: a mechanism for triggering acid explosive eruptions. *Nature* **267**, 315–18.

STAMATELOPOULOU-SEYMOUR, K., VLASSOPOULOS, D., PEARCE, T. H. & RICE, C. 1990. The record of magma chamber processes in plagioclase phenocrysts at Thera Volcano, Aegean Volcanic Arc, Greece. *Contributions to Mineralogy and Petrology* **104**, 73–84.

THOMAS, N. & TAIT, S. R. 1997. The dimensions of magmatic inclusions as a constraint on the physical mechanism of mixing. *Journal of Volcanology and Geothermal Research* **75**, 167–78.

THOMAS, N., TAIT, S. & KOYAGUCHI, T. 1993. Mixing of stratified liquids by the motion of gas bubbles: application to magma mixing. *Earth and Planetary Science Letters* **115**, 161–75.

TILLER, W. A. 1991. *The science of crystallization: macroscopic phenomena and defect generation.* Cambridge University Press, 484 pp.

TORAMARU, A. & FUJII, N. 1986. Connectivity of the melt phase in a partially molten peridotite. *Journal of Geophysical Research* **91**, 9239–52.

TURNER, J. S. & CAMPBELL, I. H. 1986. Convection and mixing in magma chambers. *Earth Science Reviews* **23**, 255–352.

VON BARGEN, N. & WAFF, H. S. 1988. Wetting of enstatite by basaltic melt at 1350 °C and 1.0–2.5 GPa pressure. *Journal of Geophysical Research* **93**, 1153–8.

WAFF, H. S. & BULAU, J. R. 1979. Equilibrium fluid distribution in an ultramafic partial melt under hydrostatic stress conditions. *Journal of Geophysical Research* **84**, 6109–14.

ZELLMER, G. F., BLAKE, S., VANCE, D., HAWKESWORTH, C. & TURNER, S. 1999. Plagioclase residence times at two island arc volcanoes (Kameni Islands, Santorini, and Soufriere, St. Vincent) determined by Sr diffusion systematics. *Contributions to Mineralogy and Petrology* **136**, 345–57.